X-911-76-192
PREPRINT

THE COVARIANCE OF TEMPERATURE AND OZONE DUE TO PLANETARY-WAVE FORCING

G. J. FRASER

SEPTEMBER 1976

GSFC — GODDARD SPACE FLIGHT CENTER —
GREENBELT, MARYLAND

X-911-76-192
Preprint

THE COVARIANCE OF TEMPERATURE AND OZONE DUE TO PLANETARY-WAVE FORCING

G. J. Fraser*
NASA/Goddard Space Flight Center
Greenbelt, Maryland 20771 USA

September 1976

*NRC/NAS Senior Resident Research Associate
Permanent address: Physics Department, University of Canterbury
Christchurch, New Zealand

GODDARD SPACE FLIGHT CENTER
Greenbelt, Maryland

THE COVARIANCE OF TEMPERATURE AND OZONE DUE TO PLANETARY-WAVE FORCING

G. J. Fraser*

NASA/Goddard Space Flight Center

Greenbelt Maryland 20771 USA

ABSTRACT

The cross-spectra of temperature and ozone mass mixing ratio at 42 km (2 mb) and 28 km (20 mb) have been determined for austral spring (1971) and summer (1971-2) over Christchurch, New Zealand (44 S, 172 E). The sources of data are the SCR and BUV experiments on Nimbus 4. The observed covariances are compared with a model in which the temperature and ozone perturbations are forced by an upward-propagating planetary wave. The agreement between the observations and the model is reasonable. It is suggested that this cross-spectral method permits an estimate of the meridional gradient of ozone mass mixing ratio from measurements of the vertical profile of ozone mass mixing ratio at one location, supported by temperature profiles from at least two locations (to determine the meridional temperature gradient).

CONTENTS

TABLES

FIGURES

1. Introduction

The availability of global measurements of stratospheric temperature and ozone from satellites is increasing our knowledge of the horizontal, vertical and temporal distribution of ozone. However, balloon-borne instrumentation is still a major source of information, particularly for the period before extensive satellite observations became available. It is, therefore, interesting to consider how much information on atmospheric motion can be deduced from the various time series of balloon observations.

The association between ozone and atmospheric temperature is commonly described in terms of eddy transport coefficients, with the implication that dynamic processes with time scales less than several months, are not measured directly and are only represented by their integrated effects. The balloon observations are usually made daily so that motion with periods of two or more days can be satisfactorily measured. It is, therefore, possible to study the ozone transport on quite short time scales and, hence, obtain an insight into the dynamical processes contributing to the eddy transport coefficients.

The temperature and the ozone concentration at a fixed point are influenced considerably by advection of horizontal gradients so that information on these gradients is essential. Although the relevant temperature gradients can usually be obtained from a group of radiosonde stations, the ozone mixing ratio gradient is seldom available.

This investigation simulates a set of balloon observations by using the satellite measurements of temperature and ozone mixing ratio at a fixed geographic location (Christchurch, New Zealand, 44 S, 172 E). The cross spectrum of the daily temperature and ozone mixing ratio measurements are calculated for austral spring (1971) and summer (1971-2). Suitable ozone data for other seasons were not available at the time of this study. The cross spectrum is then compared with that calculated from a simple model based on specified planetary wave modes. The observed seasonal mean values were used to define the atmospheric properties for the model. An attempt was then made to decide whether the meridional mixing ratio gradient could be deduced from the phase spectrum of the temperature-ozone cross-spectra.

2. The Observations

Temperature. Temperature information was taken from the Nimbus 4 SCR (Barnett et al., 1972) radiance tapes available from the Department of Atmospheric Physics, University of Oxford. The black-body equivalent of the radiance is used, i.e. the temperature of a black body which would emit the same radiance at the same wavelength. The Nimbus 4 SCR weighting functions for the two top channels have maxima near 42 km (2 mb) and 28 km (20 mb). The equivalent temperatures are weighted means over altitude regions about 20 km thick.

The Nimbus 4 satellite is sun-synchronous so that the observations are made near local noon and local midnight. The data used in the analysis was

obtained from the "gridded" tapes where all the radiances for one day have been reduced to a latitude-longitude grid, the grid points being 4° apart in latitude and 10° apart in longitude. The equivalent temperatures were obtained from daily radiances at the grid point (44 S, 172 E) closest to Christchurch, New Zealand. The mean meridional temperature gradient was calculated from the difference between the grid points (40 S, 172 E) and (48 S, 172 E).

Ozone. The ozone data was obtained from the Nimbus 4 BUV (Heath et al., 1973) results available at NASA/Goddard Space Flight Center. Vertical profiles of ozone partial pressure were given at successive locations along orbits passing near Christchurch. This BUV data is to be considered as a preliminary estimate until some inconsistencies in the data have been resolved (Krueger et al., 1973).

As the SCR weighting functions peak at [illegible] km (2 mb) and 28 km (20 mb), the ozone partial pressures for these heights were selected. The mean value and the meridional gradient were obtained by fitting a least squares plane to the data from a minimum of two orbits, one on either side of Christchurch. On the few occasions when only one orbit's data was available for a given day, the mean value and the gradient were derived from a least squares line. In this latter case there is the possibility of contamination due to zonal temperature gradients. Only data points taken within 3300 km of Christchurch were used. The ozone mass mixing ratio was derived as the ratio of ozone partial pressure to the total air pressure, multiplied by the ratio of the respective molecular weights (1.66).

Vertical Resolution. The vertical resolution of the satellite experiments is limited by the width of the weighting functions. The half-weight width of the weighting functions for the upper two Nimbus 4 SCR channels have been estimated from the published (Barnett et al., 1972) weighting function graphs to be 20 km. Similarly the BUV half-weight widths are 17-18 km for the upper five channels (Heath et al., 1973). These weighting functions will only slightly attenuate the response to a wave with a vertical wavelength whose half-wavelength is close to the half-weight width, i.e. a wave whose wavelength is 35-40 km. Waves of shorter vertical wavelengths will be resolved progressively less clearly by the satellite sensors. This is obviously a pessimistic estimate of the vertical resolution as the results from 42 and 28 km appear to be quite independent.

3. The Observed Temperature-Ozone Covariance

The spectral analysis was performed by calculating the auto- and cross-correlation functions of the appropriate pairs of time series, applying a Parzen lag window, and then taking the Fourier transforms to give the auto- and cross-spectra (Jenkins and Watts, 1969).

The occasional "wild" point was removed from the temperature and ozone data by rejecting all observations differing from the mean values by more than three sample standard deviations. The gaps, due to rejected observations and missing data, were filled by linear interpolation between values at either end of

the gap. The amount of missing data, including "wild" points, was 17% for temperatures and 31% for ozone.

The temperature data is derived from a global estimate for one day, Greenwich time, while the ozone data is obtained from individual orbits and therefore corresponds to local noon at 172 E. There is, therefore, an effective time shift of approximately 12 hours between the temperature and ozone time series. An attempt was made to remove this shift by linear interpolation between successive temperature observations. Any changes in the spectra were masked by the large fluctuations introduced in the coherence and phase spectra at the higher frequencies. This presumably occurred because the linear interpolation is equivalent to a two-point equally weighted running mean with its attendant sideband problems in the frequency domain. Consequently, the data has not been corrected for this 12 hour shift. It causes a phase displacement which is linear with frequency, 0° at 0 cycles per day (cpd) and -90° at 0.5 cpd. At the frequencies of interest in this study, (0.2 cpd and less), the phase shift is comparable with the phase confidence limits. Much of the subsequent discussion is based on the limiting value of phase as the frequency tends to zero, so the phase shift will not be significant.

The correlation functions were calculated for a maximum lag of 20 giving a maximum resolvable period of 40 days - a minimum resolvable frequency of 0.025 cpd.

The 1971 austral spring transition is included in the data selected for analysis. During this period the data will not be statistically stationary so that some

appropriate criterion was needed to distinguish spring from summer. Fortunately, an analysis of southern hemisphere temperature waves based on Nimbus 4 data was available (Harwood, 1975). Harwood found that by mid-October, 1971, there was a reduction in the amplitude of wavenumber 2 at 2 mb and a cessation of its eastward phase progression. The phase velocity of wavenumber 1 was eastward before mid-October, and westward after that time. Reversals in the meridional temperature gradient occurred at 2 mb about 28 September and at 10 mb about 23 October. Accordingly 25 October was selected as a date by which the summer circulation was established in the stratosphere. The summer data is thus likely to be stationary although the spring data will not be. February 29, 1972, was selected as the end of summer. The division into spring and summer was made after the gap-filling procedure was completed.

4. Planetary-Wave Perturbation Temperature and Velocity

The observed phase spectrum (see section 6) often appears to have a fairly simple behavior - a phase of 0° over a wide range of frequencies, or 180° at low frequencies with a drift to 0° as the frequency increases.

A simple model has been derived to see whether a comparable phase spectrum is produced by a planetary wave mode with a given zonal wave number. A simple harmonic planetary wave is assumed to propagate vertically upwards through an atmosphere whose temperature and wind speed do not change with altitude. The ozone content is defined by the mass mixing ratio. The mean

mixing ratio is assumed to vary in the vertical and north-south directions (but not in the east-west direction) to allow for vertical and meridional advection.

The finite temperature dependence of the photochemical equilibrium ozone concentration at 2 mb (Barnett, Houghton and Pyle, 1975) also requires some allowance for meridional temperature advection. A finite meridional temperature gradient is therefore included, although the mean zonal wind is assumed to be constant at all heights. This blatant contradiction of the thermal wind equation is necessary to avoid using Liouville-Green ("WKB") or numerical methods to cope with the variation of wave phase speed in the (vertical) direction of propagation which would result from a vertical variation of wind speed.

The physical variables are represented by the following symbols:

A_1 = amplitude of the perturbation stream function

B = temperature dependence of equilibrium ozone concentration

c = zonal phase velocity of the wave

f_0 = Coriolis parameter for 45 S

H = scale height

k,l,m = eastward, northward and upward wave numbers (radians m^{-1})

N = buoyancy frequency

P = atmospheric constant ($2HN^2/f_0$)

Q = ratio of horizontal to vertical advection terms

R = gas constant for air

R_e = radius of the earth

T_0 = mean temperature

T' = wave perturbation temperature

T_1 = total perturbation temperature

u_0 = mean zonal wind speed

u', v', w' = eastward, northward and upward wave perturbation velocity components

x, y, z = eastward, northward and upward displacement coordinates

X = ozone mass mixing ratio

X_0, X', X_1 = mean, perturbation and total perturbation mass mixing ratios

β = latitude dependence of Coriolis parameter

$\gamma = \frac{\partial}{\partial z}$

η = temperature coefficient of equilibrium ozone mass mixing ratio

ϕ = cross-spectral phase

ψ' = wave perturbation stream function

ω = wave angular frequency

In mathematical form the assumptions of the model are:

$$\frac{\partial u_0}{\partial x} = 0 \qquad \frac{\partial T_0}{\partial x} = 0 \qquad \frac{\partial X_0}{\partial x} = 0$$

$$\frac{\partial u_0}{\partial t} = 0 \qquad \frac{\partial u_0}{\partial y} = 0 \qquad \frac{\partial u_0}{\partial z} = 0$$

$$\frac{\partial T_0}{\partial t} = 0 \qquad \frac{\partial T_0}{\partial z} = 0$$

The wave properties can be deduced by substituting the above assumptions in the equation for the quasi-geostrophic perturbation potential vorticity on a mid-latitude β-plane in the absence of heating and the equation for the thermodynamic balance (Charney 1973, Holton 1975).

$$\left(\frac{\partial}{\partial t}+u_0\frac{\partial}{\partial x}\right)\left[\nabla^2\psi'+(f_0^2/N^2)\left(\frac{\partial^2\psi'}{\partial z^2}-\frac{1}{H}\frac{\partial\psi'}{\partial z}\right)\right]+\beta\frac{\partial\psi'}{\partial z}=0 \tag{1}$$

$$\left(\frac{\partial}{\partial t}+u_0\frac{\partial}{\partial x}\right)\frac{\partial\psi'}{\partial z}+(N^2/f_0)w'=0 \tag{2}$$

We assume the perturbation stream function appropriate to a simple harmonic plane wave

$$\psi'=A_1\exp\left[i(kx+\ell y+mz-\omega t)+z/2H\right] \tag{3}$$

It is convenient to define

$$\gamma=im+1/2H$$

so that

$$\frac{\partial\psi'}{\partial z}=\gamma\psi' \tag{4}$$

Substituting (3) and (4) in (1) we obtain

$$\left\{(\omega-ku_0)\left[(k^2+\ell^2)+(f_0^2/N^2)(m^2+1/4H^2)\right]+\beta k\right\}\psi'=0 \tag{5}$$

Eq. (5) has a non-trivial solution if

$$\omega = ku_0 - \beta k/[(k^2 + \ell^2) + (f_0^2/N^2)(m^2 + 1/4H^2)] \tag{6}$$

Eq. (6) is the required dispersion equation from which we derive the horizontal phase velocity

$$c = \omega/k = u_0 - \beta/[(k^2 + \ell^2) + (f_0^2/N^2)(m^2 + 1/4H^2)] \tag{7}$$

The vertical wave number is given by

$$m^2 = (N^2/f_0^2)[\beta/(u_0 - c) - (k^2 + \ell^2)] - 1/4H^2 \tag{8}$$

The vertical group velocity is

$$\frac{\partial \omega}{\partial m} = 2\beta f_0^2 N^2 mk/[N^2(k^2 + \ell^2) + f_0^2(m^2 + 1/4H^2)] \tag{9}$$

The vertical group velocity gives the appropriate sign for the vertical wave number (m) in (8). It will be assumed that energy is propagating upwards through the region; the vertical (m) and zonal (k) wave numbers must then have the same sign.

From the stream function we obtain the horizontal perturbation velocity components and the perturbation temperature:

$$u' = -i\ell\psi' \tag{10}$$

$$v' = ik\psi' \tag{11}$$

$$T' = (f_0/R)\frac{\partial \psi'}{\partial z} = (\gamma f_0/R)\,\psi' \tag{12}$$

From the thermodynamic equation (2) and from (4) we have the vertical perturbation velocity

$$w' = i(\gamma f_0/N^2)\,(\omega - ku_0)\,\psi' \tag{13}$$

$$= i(R/N^2)\,(\omega - ku_0)T' \tag{14}$$

Eqs. (4), (11), and (12) give the relationship between the meridional perturbation velocity and the perturbation temperature

$$v' = i(kR/\gamma f_0)T'. \tag{15}$$

5. A Simple Model For Temperature-Ozone Covariance

The rate of change of ozone mass mixing ratio is

$$\frac{dX}{dt} = \frac{\partial X}{\partial t} + v'\frac{\partial X}{\partial y} + w'\frac{\partial X}{\partial z} \tag{16}$$

Substituting (14) and (15) in (16) we have

$$\frac{dX}{dt} = \frac{\partial X}{\partial t} + i\left(\frac{\partial X}{\partial y}\right)\left(\frac{kR}{\gamma f_0}\right)T' + i\left(\frac{\partial X}{\partial z}\right)\left(\frac{R}{N^2}\right)(\omega - ku_0)T' \tag{17}$$

Eq. (17) contains the basic principle of this analysis — that the phase difference between the ozone and temperature variations depends on a combination of atmospheric and wave parameters. It should therefore be possible to deduce some atmospheric parameters from the frequency dependence of the phase difference

between temperature and ozone perturbations, supported by assumptions or measurements of the wave parameters.

The time-dependent term in (16) and (17) would be zero if the ozone mass mixing ratio was a conservative property of the atmosphere. Even if photochemical equilibrium is assumed there still remains the temperature dependence of the equilibrium mixing ratio. From the discussion by Barnett, Houghton and Pyle (1975) on the temperature dependence of the ozone concentration near the stratopause it is estimated that near 2 mb (42 km) the mixing ratio will behave like exp (B/T), where B ~1000 K. Consequently, the temperature coefficient of the ozone mass mixing ratio is

$$\eta = \frac{1}{X}\frac{\partial X}{\partial T} = -B/T^2 \tag{18}$$

Hence

$$\frac{\partial X}{\partial t} = \frac{\partial X}{\partial T}\frac{dT}{dt} = \eta X \frac{dT}{dt} \tag{19}$$

Let the mixing ratio be

$$X = X_0 + X_1$$

where

$$X_1 \sim \exp(-i\omega t) \tag{20}$$

Therefore

$$\frac{dX}{dt} = -i\omega X_1 \tag{21}$$

Combining (11), (13), (16), (19), (20) and (21), and neglecting the spatial gradient of the perturbation mixing ratio, we have

$$-i\omega X_1 = \eta X_0 \frac{dT}{dt} + \frac{\partial X_0}{\partial y} (ik\psi') + i(\gamma f_0/N^2)(\omega - ku_0)\psi' \tag{22}$$

The time-dependent temperature term will contain a direct contribution from the wave perturbation temperature and another from the advective heating. The temperature is

$$T = T_0 + T_1$$

where

$$T_1 \sim \exp(-i\omega t)$$

Therefore

$$\frac{dT}{dt} = \frac{\partial T'}{\partial t} + v' \frac{\partial T_0}{\partial y} \tag{23}$$

From (12)

$$\frac{\partial T'}{\partial t} = -i\omega(\gamma f_0/R)\psi'$$

Consequently

$$\frac{dT_1}{dt} = -i\omega T_1$$

$$= -i\omega(\gamma f_0/R)\psi' + i\frac{\partial T_0}{\partial y} k\psi' \tag{24}$$

and

$$T_1 = (\gamma f_0/R)\psi' - (k/\omega)\frac{\partial T_0}{\partial y}\psi' \tag{25}$$

Substituting (24) in (22) we obtain

$$-i\omega X_1 = \eta X_0 \left[-i\omega\gamma(f_0/R)\psi' + i\frac{\partial T_0}{\partial y} k\psi'\right] + i\frac{\partial X_0}{\partial y} k\psi' + i\gamma(f_0/N^2)(\omega - ku_0)\psi'$$

so that

$$X_1 = [\gamma X_a + (X_s + X_h)/\omega + \gamma X_v(u_0 - c)/\omega]\ \psi' \tag{26}$$

where

$$X_a = \eta X_0(f_0/R)$$

$$X_h = -k\frac{\partial X_0}{\partial y}$$

$$X_s = -k\eta X_0\frac{\partial T_0}{\partial y}$$

$$X_v = k(f_0/N^2)\frac{\partial X_0}{\partial z}$$

These four terms represent the changes in ozone mass mixing ratio due to, respectively, the direct temperature change from wave perturbation, horizontal advection of the mixing ratio gradient, the temperature change from horizontal temperature advection, and vertical advection of the mixing ratio gradient.

Similarly the temperature change (25) is the sum of two terms

$$T_1 = \gamma T_a \psi' + (T_h/\omega)\psi' \tag{27}$$

where $T_a = f_0/R$, a direct perturbation term and $T_h = -k\ \partial T_0/\partial y$, an advective term.

The covariance of temperature and mixing ratio is then

$$\begin{aligned} C(T, X, \omega) &= T_1 X_1^* \\ &= [\gamma T_a + T_h/\omega]\ [\gamma^* X_a + (X_s + X_h)/\omega + \gamma^* X_v (u_0 - c)/\omega]\ \psi' \psi'^* \end{aligned} \tag{28}$$

The perturbations, T_1 and X_1, are simple harmonic terms so that the coherence spectrum is of little interest, being perfect (1. 0) at all frequencies. However the phase spectrum ($\phi(\omega)$) does contain information.

$$\phi(\omega) = \tan^{-1} (C_i\ (T, X, \omega)/C_r\ (T, X, \omega)) \tag{29}$$

where

C_r = real part of $C(T, X, \omega)$

C_i = imaginary part of $C(T, X, \omega)$.

In a homogeneous atmosphere

$$\frac{\partial X_0}{\partial z} = 0 \qquad \text{and} \qquad \frac{\partial X_0}{\partial y} = 0$$

and the numerator of (28) is zero. The sign of the denominator depends only on the sign of η, which is a negative number. Consequently, $\phi(\omega) \equiv 180°$. The correlation coefficient between the two simple harmonic variables is then $\cos(\phi(\omega)) = -1.0$.

Wherever $\phi \sim 90°$, the correlation coefficient will be very small, even if the coherence is perfect. Consequently, it is inadvisable to use the correlation coefficient to express the relationship between quasi-periodic variables; an insignificant correlation coefficient does not necessarily imply a lack of dependence — it may merely indicate a phase difference close to 90°.

6. Comparison of the Model and Observed Covariances

In relating the model to observed covariances, the number of free parameters has been minimized by taking the mean temperature and the mean mass mixing ratio and their respective gradients from the data itself. The values used are given in Table 1. Where magnitudes did not differ greatly from each other, a representative value was selected to simplify comparsions. For instance, the summer meridional temperature gradients at 2 and 20 mb were -2.5 and +3.0 K over 10° of latitude, while the 20 mb spring gradient was +1.3K over 10° of latitude. A magnitude of 2 K over 10° of latitude was therefore chosen, with the appropriate signs, for each of these values.

The 2 mb observations represent conditions of approximate photochemical equilibrium, with a known temperature dependence of the ozone concentration (Barnett, Houghton and Pyle, 1975). Conversely, the equilibrium time at 20 mb is of the order of months (Nicolet, 1975) so that on the time scales relevant here, only advective changes need be considered. This is achieved by setting to zero the value of the temperature coefficient of the ozone mass mixing ratio at 20 mb.

The selection of suitable zonal winds is also difficult as there is considerable variation in the spring, and some variation during the four summer months. Calculations with a wide range of model parameters confirmed that the dominant effect of the wind is to determine when a given wave mode becomes evanescent, through the $(u_0 - c)$ term in (8). The wind speed also appears in the $(u_0 - c)$ term of (28). As the wind speed is always associated with wave number and with the independent variable ω in

$$(u_0 - c) = (u_0 - \omega/k),$$

it is possible to qualitatively estimate the effect of a wind speed change from the consequent changes in ω and k necessary to maintain a given value of $(u_0 - c)$. The model assumes a typical wind speed of 20 m sec^{-1}, the direction being eastward in the spring and westward in the summer at both 2 and 20 mb.

In this preliminary study, no observational estimate of the meridional wave number was sought, so a value of zero was selected, making this model

consistent with that of Hirota (1971). Holton (1975) discusses the problems of meridional scale and polar boundary values in the β-plane approximation.

The observed 2 mb spring phase spectrum (Fig. 1) tends to a limiting value of about 215° at low frequencies. This behavior is consistent with the model and suggests that the limiting phase angle (as the frequency decreases to zero) may have some significance, despite the fact that the periods greater than 40 days are not directly observable. From (29) it can be shown that

$$\lim_{\omega \to 0} \phi(\omega) = \tan^{-1} 2m_0 H/((PQ/u_0) - 1) \qquad (30)$$

where

$$m_0 = \lim_{\omega \to 0} m \text{ (equation 8)}$$

$$P = 2HN^2/f_0$$

$$Q = \left(\eta \frac{\partial T_0}{\partial y} + \frac{1}{X_0} \frac{\partial X_0}{\partial y}\right) \Big/ \left(\frac{1}{X_0} \frac{\partial X_0}{\partial z}\right)$$

The product PQ is independent of the wave number and comprises a constant P (-6×10^4 m sec^{-1} in this model) and a dimensionless number (Q) which is the ratio of the horizontal to vertical advection terms.

The limiting vertical wave number (m_0) does depend on the zonal wave number through (8). However, the consequent variation in phase is not great, as shown in Table 2.

Eq. (30) shows that the limiting phase is controlled by the ratio (Q) of horizontal to vertical advection terms. For instance, if there is no vertical ozone gradient, the limiting phase angle will be 0 or 180 , depending on the relative magnitudes of the horizontal temperature and ozone advection terms. This is in agreement with the phase difference between meridional displacement and perturbation temperature calculated from (15). Around 20 mb and below, Q will simply be the ratio of horizontal to vertical ozone gradients as the equilibrium time is so long.

The summer phase spectrum at 2 mb (Fig. 2) is not significantly different from 180° for frequencies less than 0.15 cpd. Thereafter, the phase decreases, but the phase fluctuations increase as the coherence decreases. This behavior is also consistent with the model, although the 180° phase angle there corresponds to the evanescent model.

Hirota (1975) reported a westward moving vertically propagating wave number 1 mode in the southern hemisphere for summer 1972-3. This is consistent with the trend in Harwood's (1975) analysis for October 1971. Hirota also reported eastward moving waves with wave numbers 2 and 3 and suggested that these might be evanescent modes as $(u_0 - c)$ was negative. The phase speed of the westward mode was -28 m sec^{-1} at 30 S and -16 m sec^{-1} at 60 S. It would therefore be about -22 m sec^{-1} at 44 S but the mean zonal wind is not given, so no comparison can be made with this model, but if the wind were comparable with that assumed for this model, the wave mode would be close to evanescence (and therefore close to the maximum response to a given amplitude of lower

boundary forcing — see Hirota, 1971). However, the experimentally observed low frequency phase is best explained by an evanescent mode in the model as the propagating modes have phase differences of about 90° near their low frequency limit.

The 20 mb spring phase spectrum (Fig. 3) is not significantly different at low frequencies from that predicted by the model. The 20 mb summer phase spectrum is not considered, as the coherence spectrum nowhere reached the 95% significance level, presumably because the westward winds suppressed propagation.

7. Conclusion

In principle, then, ozone measurements by balloon from one location could provide an estimate of the meridional ozone gradient, provided there are enough temperature observations to determine the meridional temperature gradient. The feasibility of this approach will need more extensive analysis of (30) with various gradients and due allowance for the confidence limits of observable phase. The latter depend in turn on the coherence spectrum. The coherence and phase are amplitude-independent and give no indication of the amount of energy at the various frequencies; the cross-amplitude spectrum is therefore essential to any discussion of relative energy contributions of the various wave modes. The model will then require modification to include the dependence of forced amplitude on the vertical wave number (Hirota, 1971) and consequent assumptions

about the spatial and temporal spectra of the forcing perturbation at the lower boundary.

It is also necessary to confirm the assumption that the temperature and ozone perturbations are due to the same planetary wave. This study must await the availability of ozone data for several seasons around a latitude circle.

The summer phase spectra and Hirota's (1975) results imply that evanescent modes need to be considered more closely; this will require a more careful examination of boundary conditions and the direction of energy propagation than has been assumed here for propagating modes.

A further and highly desirable extension of this study is to see whether the principle exemplified by (30) can be extended to total ozone measurements made by a ground-based u. v. spectrophotometer at one location.

Acknowledgements. This study was begun during a visit to the Department of Atmosphereic Physics, University of Oxford, and completed during a visit to NASA/Goddard Space Flight Center. I wish to thank Dr. J. T. Houghton (Oxford University) for making available the Nimbus 4 SCR data, and Dr. D. F. Heath (NASA/GSFC) for making available the Nimbus 4 BUV data. I am grateful to members of both institutions, particularly Dr. J. J. Barnett (Oxford University) and Mr. John S. Theon (NASA/GSFC) for many helpful discussions. The visits were made possible by financial assistance from the University of Canterbury (New Zealand) and the U. S. National Academy of Sciences.

References

Barnett, J. J., Cross, M. J., Harwood, R. S., Houghton, J. T., Morgan, C. G., Peckham, G. E., Rodgers, C. D., Smith, S. D. and Williamson, E. J., 1972: The first year of the selective chopper radiometer on Nimbus 4. Quart. J. Roy. Meteor. Soc., 98, 17-37.

Barnett, J. J., Houghton, J. T. and Pyle, J. A., 1975: The temperature dependence of the ozone concentration near the stratopause. Quart. J. Roy. Meteor. Soc., 101, 245-257.

Charney, J. G., 1973: Planetary fluid dynamics., in P. Morel (ed.): Dynamic meteorology, Dordrecht, Reidel.

Harwood, R. S., 1975: The temperature structure of the southern hemisphere stratosphere, August-October 1971. Quart. J. Roy. Meteor. Soc., 101, 75-91.

Heath, D. F., Mateer, C. L., and Krueger, J. A., 1973: The Nimbus-4 backscatter ultraviolet (BUV) atmospheric ozone experiment — two years' operation. Pure and Appl. Geophys., 106-108, 1238-1253.

Hirota, I., 1971: Excitation of planetary Rossby waves by periodic forcing. J. Meteor. Soc. Japan, 49, 439-448.

Hirota, I., 1975: Spectral analysis of planetary waves in the summer stratosphere and mesosphere. J. Meteor. Soc. Japan, 53, 33-44.

Holton, J. R., 1975: The dynamic meteorology of the stratosphere and mesosphere. (Meteorological Monographs, 15, No. 37), Boston, American Meteorological Society.

Jenkins, G. M. and Watts, D. G., 1968: Spectral Analysis and its Applications. San Francisco, Holden-Day.

Krueger, A. J., Heath, D. F. and Mateer, C. L., 1973: Variations in the stratospheric ozone field inferred from Nimbus satellite observations. Pure and Appl. Geophys., 106-108, 1254-1263.

Nicolet, M., 1975: Stratospheric ozone: an introduction to its study. Rev. Geophys., 13, 593-636.

Table 1

Observed Mean Values Used as Model Parameters

Height	Season	$\frac{\partial T_0}{\partial y}$	$\frac{\partial X_0}{\partial y}$	$\frac{\partial X_0}{\partial z}$
42 km (2 mb)	spring	-6 K/10° lat.	$+10^{-12}$ m^{-1}	-10^{-9} m^{-1}
42 km (2 mb)	summer	-2	-10^{-13}	-10^{-9}
28 km (20 mb)	spring	+2	$+2 \times 10^{-12}$	-3×10^{-10}
28 km (20 mb)	summer	-2	$+10^{-13}$	-3×10^{-10}

Table 2

Low Frequency Limit Of Model Phase Spectrum in Spring

Height	Zonal Wave Number					
	-3	-2	-1	-1	+2	+3
42 km (2 mb)	157°	148°	144°	216°	212°	203°
28 km (20 mb)	356°	354°	353°	7°	6°	4°

Positive zonal wave numbers indicate eastward-moving waves; negative zonal wave numbers indicate westward-moving waves.

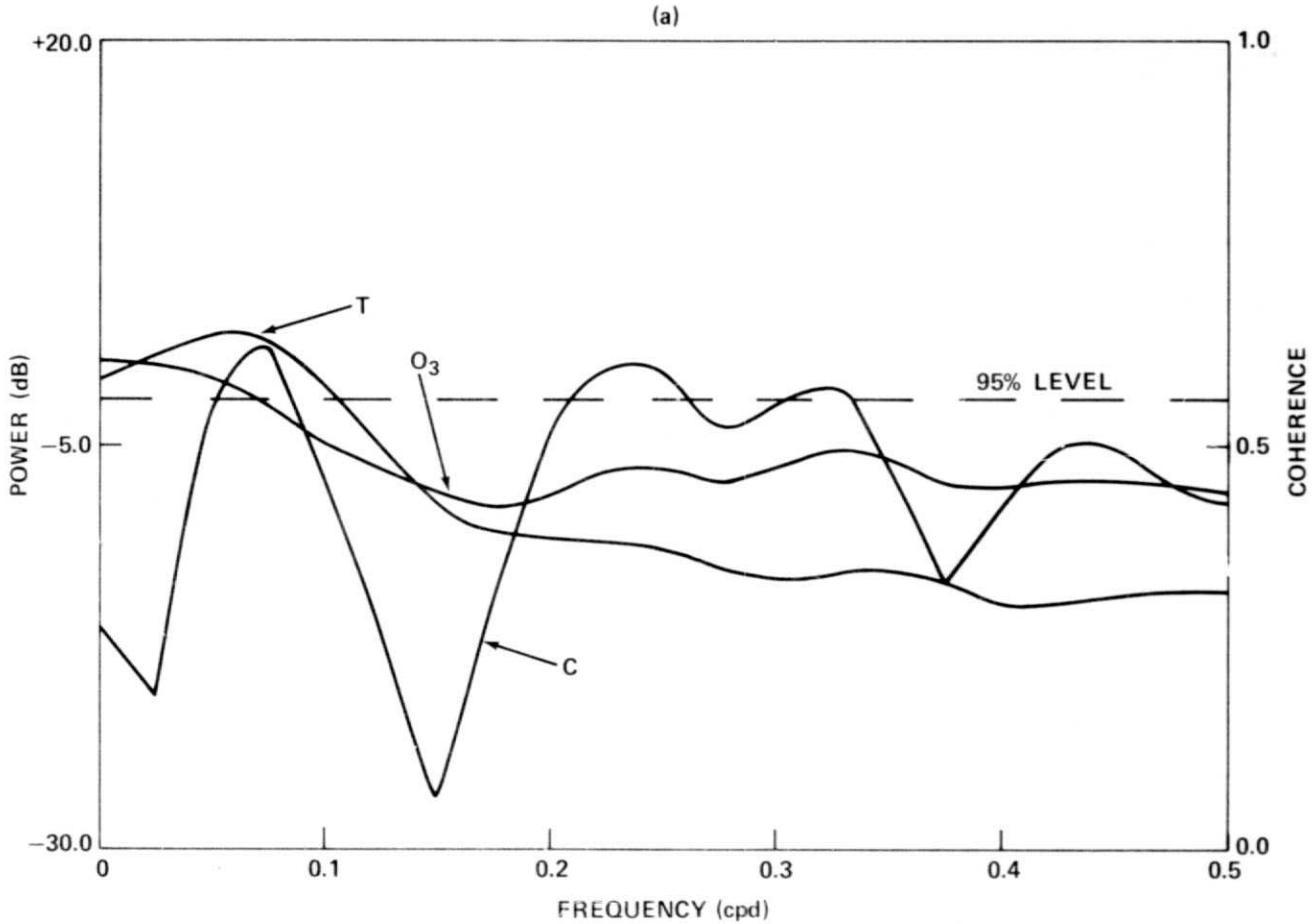

Figure 1a Data for 2 mb, spring 1971. Power spectra for temperature (T) and ozone mass mixing ratio (0_3), and the coherence spectrum (C). Power is in decibels relative to the total variance about the mean. The 95% significance level is for coherence.

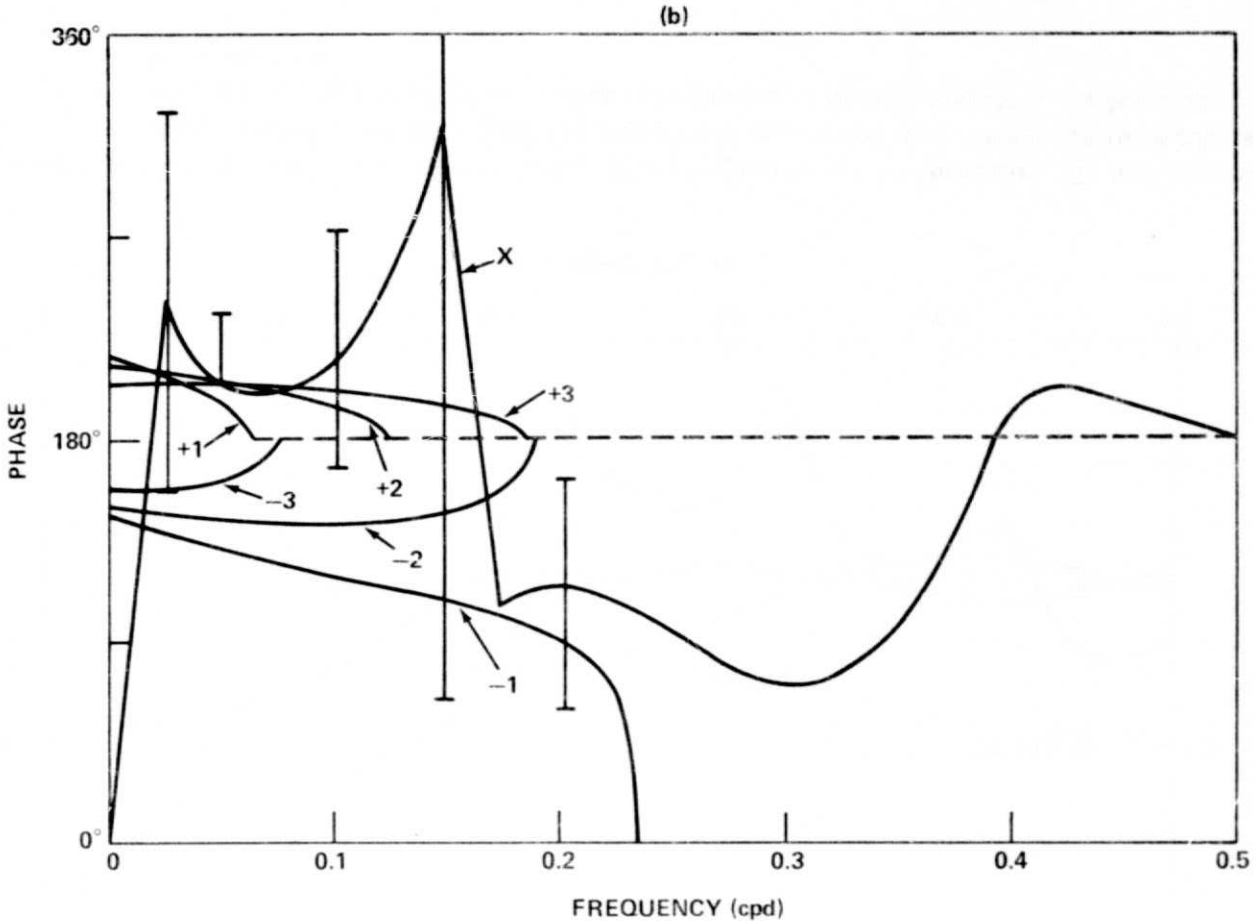

Figure 1b Data for 2 mb, spring 1971. The observed phase spectrum is marked X, and some 95% confidence limits are indicated. The curves labelled +n (or -n) are the spectra calculated from the model for eastward (or westward) travelling modes with wave number n. Evanescence is indicated by the dashed line.

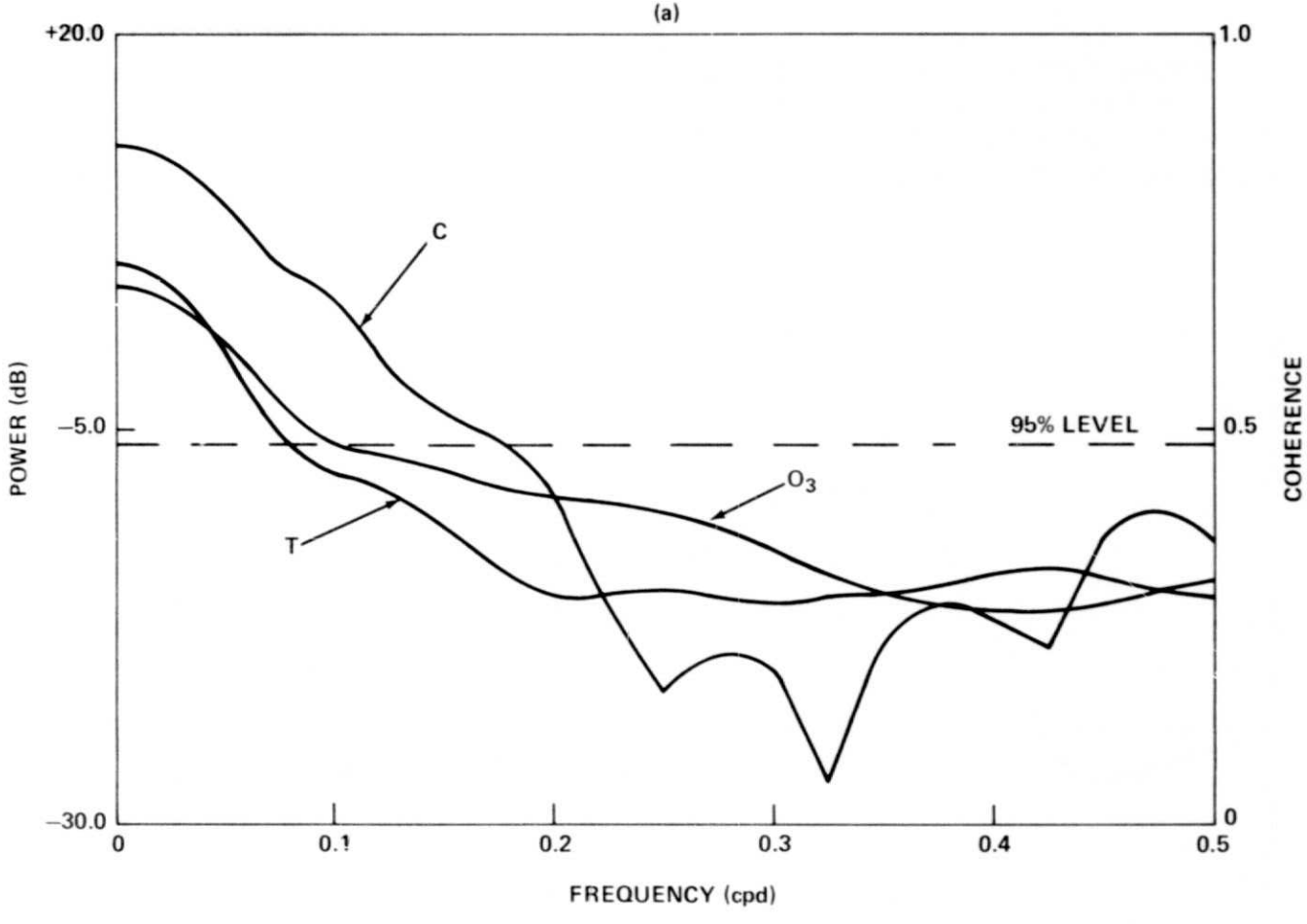

Figure 2a Data for 2mb, summer 1971-2. Power spectra for temperature (T) and ozone mass mixing ratio (0_3), and the coherence spectrum (C). Power is in decibels relative to the total variance about the mean. The 95% significance level is for coherence.

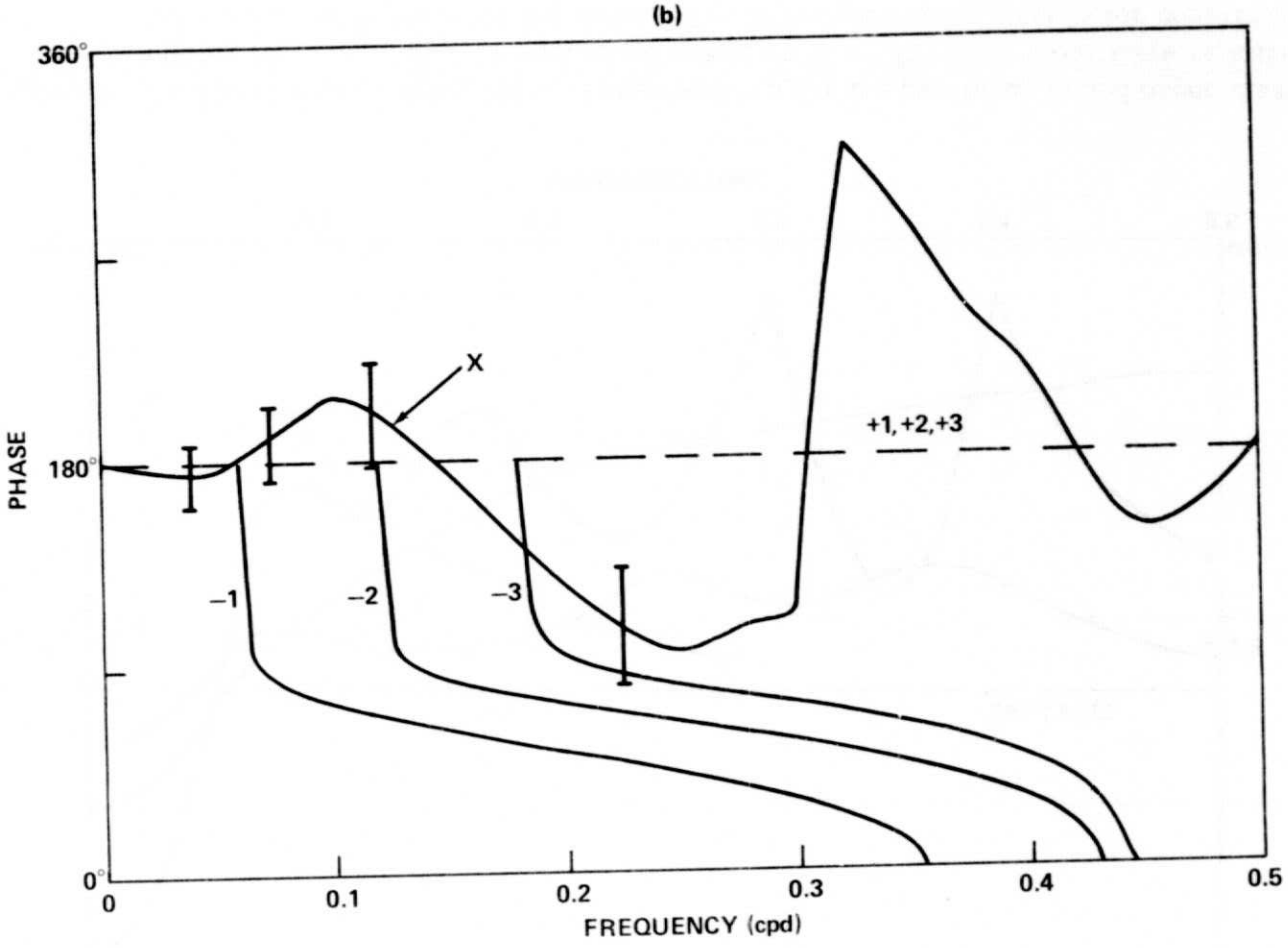

Figure 2b Data for 2 mb, summer 1971-2. The observed phase spectrum is marked X, and some 95% confidence limits are indicated. The curves labelled +n (or -n) are the spectra calculated from the model for eastward (or westward) travelling with wave number n. Evanescence is indicated by the dashed line.

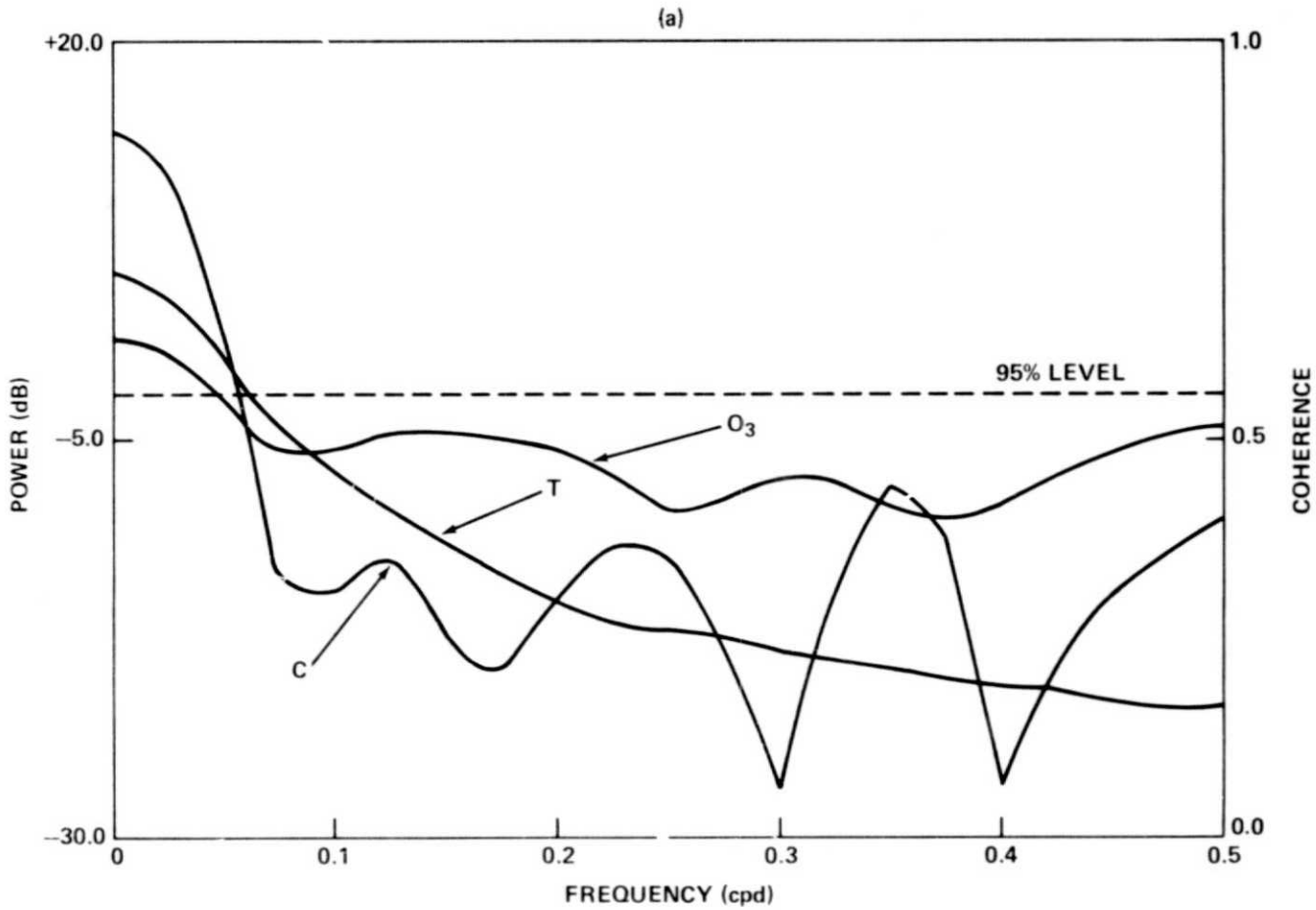

Figure 3a Data for 20 mb, spring 1971. Power spectra for temperature (T) and ozone mass mixing ratio (0_3), and the coherence spectrum (C). Power is in decibels relative to the total variance about the mean. The 95% significance level is for coherence.

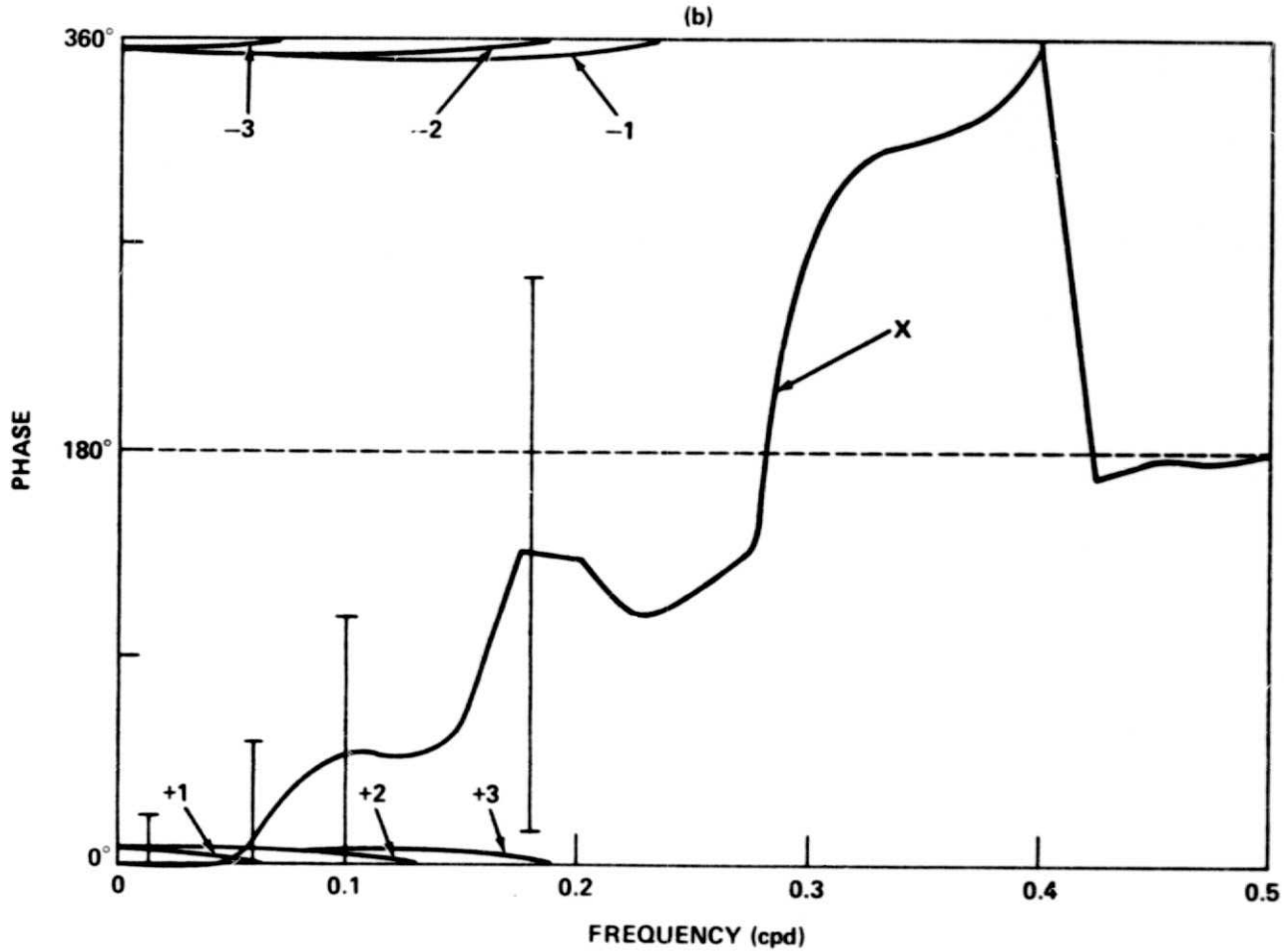

Figure 3b Data for 20 mb, spring 1971. The observed phase spectrum is marked X, and some 95% confidence limits are indicated. The curves labelled +n (or -n) are the spectra calculated from the model for eastward (or westward) travelling modes with wave number n. Evanescence is indicated by the dashed line.